Miscibility of phospholipids with identical headgroups and acyl chain lengths differing by two methylene units: Effects of headgroup structure and headgroup charge. Biochim. Biophy...

ARTICLE *in* BIOCHIMICA ET BIOPHYSICA ACTA · APRIL 1998

Impact Factor: 4.66 · DOI: 10.1016/S0005-2736(98)00005-4 · Source: PubMed

2 AUTHORS:

Patrick Garidel
Martin Luther University Halle-Wittenberg
148 PUBLICATIONS **3,154** CITATIONS
SEE PROFILE

Alfred Blume
Martin Luther University Halle-Wittenberg
252 PUBLICATIONS **7,305** CITATIONS
SEE PROFILE

ELSEVIER

Biochimica et Biophysica Acta 1371(1998) 83–95

BIOCHIMICA ET BIOPHYSICA ACTA
BBA

Miscibility of phospholipids with identical headgroups and acyl chain lengths differing by two methylene units: Effects of headgroup structure and headgroup charge

Patrick Garidel [a], Alfred Blume [a,b,*]

[a] *Fachbereich Chemie, Universität Kaiserslautern, D-67653 Kaiserslautern, Germany*
[b] *Institut für Physikalische Chemie, Martin-Luther-Universität Halle-Wittenberg, D-06108 Halle / Saale, Germany*

Received 20 October 1997; accepted 13 January 1998

Abstract

We have investigated the influence of the chemical structure and charge of the hydrophillic headgroup on the miscibility of saturated phospholipids with acyl chain lengths differing by two methylene units, namely DMPA/DPPA, DMPC/DPPC, DMPE/DPPE and DMPG/DPPG (0.1 M NaCl). All four mixtures were analysed by DSC at pH 7. To study the influence of a change in headgroup charge, we additionally investigated DMPA/DPPA mixtures at pH 4 and 12, and DMPG/DPPG mixtures at pH 2. The experimental DSC thermograms were fitted using methods described before [Johann et al., Biophys. J. 71 (1996), 3215–3228] to obtain the temperatures of onset and end of melting and first approximations for the non-ideality parameters as a function of composition. The resulting phase diagrams were then fitted using a four non-ideality parameter model for non-ideal, non-symmetric mixing in both phases. The phase diagram of the system DMPG/DPPG has a lens-like shape, the non-ideality parameters ρ_g and ρ_l for the gel and the liquid-crystalline phase, respectively, are zero, indicating ideal mixing in both phases. For the other mixtures, differences in miscibility are observed depending on the structure of the headgroup. At pH 7, $\rho_g > \rho_l$, i.e., the miscibility in the liquid-crystalline phase is more ideal than in the gel state. All ρ_g values are positive and the sequence for ρ_g observed is PA > PE > PC > PG. Partial protonation of PA at pH 4 or complete deprotonation at pH 12 leads to negative non-ideality parameters for both phases, indicating a preference for mixed pair formation. Protonation of PG in DMPG/DPPG mixtures at pH 2 leads to positive non-ideality parameters for both phases, indicating a tendency for demixing. The results show, that the miscibility of phospholipids with identical headgroups but chain lengths differing by two methylene groups is dependent on headgroup structure and on headgroup charge. © 1998 Elsevier Science B.V.

Keywords: DSC; Phospholipid; Pseudobinary lipid mixture; Phase diagram; Non-ideal mixing; Non-ideality parameter

1. Introduction

The general structure of biological membranes is usually described using the so called ‘fluid mosaic model’ of Singer and Nicolson [1], where intrinsic

* Corresponding author. Institut für Physikalische Chemie, Martin-Luther-Universität Halle-Wittenberg, Mühlpforte 1, D-06108 Halle/Saale, Germany. Fax: +49-345-552-7157; E-mail: blume@chemie.uni-halle.de

PII S0005-2736(98)00005-4

proteins are embedded in a liquid-crystalline lipid bilayer and peripheral proteins interact through polar interaction forces with the surface of the lipid bilayers. The lipid bilayer is composed of a complex mixture of different lipids and evidence is accumulating that domain formation in the plane of the membrane is possible, providing different intrinsic proteins with their specific lipid surrounding for optimal function [2–19]. Studies of the mixing behaviour of different lipids in hydrated liquid-crystalline bilayers become therefore very important. In order to better understand lipid miscibility and non-ideality of mixing, an approach using simple model systems is appropriate.

Many investigations mentioned above have been reported on the mixing behaviour of so called 'pseudobinary' lipid mixtures, where the term 'pseudobinary' refers to the fact that in addition to both lipid components, a large excess of water is present in the system as a third component. Therefore in reality we are dealing with a ternary system. However, because the amount of water of the lipid phases remains almost constant, this ternary system can in an approximation be reduced to a 'pseudobinary' system [20].

Among different classes of phospholipids, mixtures of phosphatidylcholines (PC) and phosphatidylethanolamines (PE) have been studied thoroughly [21–35] because of their large abundance as membrane constituting lipids. Also, mixtures containing phosphatidic acids (PA) have been investigated [36–38], and mixtures of PC and phosphatidylglycerols (PG) have been studied intensively by several groups [39,40].

The mixing behaviour of different components is reflected in the shape of the phase diagram of the mixture, i.e., the curvature and the separation of the coexistence lines. In most cases studied so far, non-ideal mixing with a tendency for demixing or even complete immiscibility was mainly observed for the gel state bilayers, but recently we also found mixtures where demixing can be found for the liquid-crystalline phase [38,40]. The lipid miscibility depends on the difference in headgroup structure and charge, as well as on the difference in chain length and the type of acyl chains of the lipids. Also, the mixing properties depend on the bilayer phase structure, i.e., whether it is in the gel or the liquid-crystalline phase and whether tilted or non-tilted gel phases are present. Usually, mixing in the liquid-crystalline phase is more ideal due to the fluid nature of the L_α-phase.

The miscibility of two lipids (A and B) depends on the difference in pair interaction energies among the like pairs (A–A or B–B) and mixed pairs (A–B) in a mixture. In the case of ideal mixing of two lipids, the interactions of like pairs and mixed pairs are the same. The phase boundaries (*solidus* and *liquidus* lines) enclose a lens-like two-phase region in the temperature versus mole fraction diagram. The extent of deviations from ideal behaviour can be expressed in terms of non-ideality parameters ρ, determining the excess free energies of mixing [20]. A positive ρ is an indication for the tendency of clustering of like molecules while for negative ρ-values mixed pairs (AB) are preferred.

Experimental data for the construction of phase diagrams are easily obtained by calorimetry (DSC) of dilute aqueous suspensions of multilamellar liposomes of lipid mixtures. A major problem is the correct determination of the temperatures which describe the beginning and end of melting of a mixture, i.e., the temperature values from which the *solidus* and *liquidus* curves of the phase diagram are constructed. Empirical methods [24,40] have a certain arbitrariness. Therefore we have developed a method which is able to find the temperatures for onset and end of the phase transition by simulating the experimental heat capacity curves obtained by DSC. These temperature data are then used for the construction of the phase diagrams by using a four parameter regular solution model [20,38,40]. In the course of these studies we found considerable differences in the mixing behaviour of phospholipids which form identical gel phases when the headgroups are exchanged. For instance, mixtures of DMPC/DPPG behave differently compared to those of DMPG/DPPC, and even when the chain lengths of both lipids are the same, the mixing properties change with chain length, i.e., DMPC/DMPG has a different mixing behaviour compared to DPPC/DPPG [40].

In this study we have therefore examined pseudobinary systems at pH 7, where both lipids have the same headgroup, but different chain lengths, namely DMPA/DPPA, DMPC/DPPC, DMPE/DPPE and DMPG/DPPG. The DMPA/DPPA system was additionally analysed at pH 4 and pH 12 and DMPG/DPPG mixtures at pH 2, to study the influ-

ence of a change in headgroup charge. We will show that the miscibility parameters are different for these four systems when they are at pH 7 and that for PG and PA mixtures they are also dependent on the ionisation state of the headgroup.

2. Materials and methods

1,2-Dimyristoyl-*sn*-glycero-3-phosphatidic acid (DMPA), 1,2-dimyristoyl-*sn*-glycero-3-phosphorylcholine (DMPC), 1,2-dimyristoyl-*sn*-glycero-3-phosphorylglycerol (DMPG, Na-salt), 1,2-dimyristoyl-*sn*-glycero-3-phosphorylethanolamine (DMPE), 1,2-dipalmitoyl-*sn*-glycero-3-phosphatidic acid (DPPA), 1,2-dipalmitoyl-*sn*-glycero-3-phosphorylcholine (DPPC), 1,2-dipalmitoyl-*sn*-glycero-3-phosphorylglycerol (DPPG, Na-salt) and 1,2-dipalmitoyl-*sn*-glycero-3-phosphorylethanolamine (DPPE) were obtained from Nattermann Phospholipid (Cologne, Germany) and from Lipoid (Ludwigshafen, Germany). The purity of the lipids was checked by thin-layer chromatography (TLC) using a phosphorous sensitive spray and charring with concentrated sulfuric acid. The compounds were $\approx 99\%$ pure as determined by TLC (only one spot was detected on the TLC-plate) and therefore used without further purification.

Lipid stock solutions in $CHCl_3$:CH_3OH (2:1, v:v) of the different lipids were prepared and then mixed in appropriate quantities to obtain the desired molar ratios. The solvent was rapidly removed under an argon stream by carefully heating the samples. The dried mixtures were then held for 24 h under high vacuum to remove residual traces of solvent. After drying, the appropriate amount of ultra pure water (Reinstwassersystem RS 90-4 MF, Barsbüttel, Germany) for PA, PC and PE systems or aqueous 0.1 M NaCl for PG was added and the samples were vigorously vortexed for 5 min at 10 to 15°C above the main phase temperature of the mixture and additionally for 5 min at room temperature to get a homogeneous dispersion (this procedure was repeated three times). This leads to dispersions of multilamellar vesicles in excess water. The pH of the samples was checked and corrected with an appropriate amount of HCl or NaOH. DSC measurements of DMPA/DPPA mixtures were performed at pH 4, pH 7 and pH 12, for DMPG/DPPG mixtures (0.1 M NaCl) at pH 2 and pH 7, and of DMPC/DPPC and DMPE/DPPE at pH 7. The total lipid concentration was 2.5 mg/ml. The pH was measured before and after each DSC experiment. No change of pH was observed.

DSC measurements were performed using a MicroCal MC-2 differential scanning calorimeter (MicroCal, Northampton, MA, USA). A heating rate of 1°C/min was used and the measurements were performed in the temperature interval from 8°C to 85°C. For a check of the reproducibility three scans were usually recorded. After the measurements the samples were checked by TLC and no degradation of the lipids was detected. At pH 12 and at pH 2 only the first scan was used for evaluation because of some hydrolysis of the lipids at these extreme pH values as detected by TLC after the second run. Three different samples were investigated for each composition. The experimental data were evaluated using the Origin software package as supplied by MicroCal. The accuracy for the main phase transition temperature T_m was ± 0.1°C and for the main transition enthalpy $\Delta H_m \pm 0.2$ kcal/mol.

3. Theory and simulation methods

The theory and the simulation methods have been described in detail in previous publications [20,38]. Briefly, the experimental cp curves are simulated using a model based on regular solution theory with the additional incorporation of a broadening function taking into account the reduced cooperativity in mixed lipid bilayers [47]. Output parameters of these simulations are two non-ideality parameters ρ for describing non-ideal mixing in the gel and the liquid-crystalline phase, the temperatures $T(-)$ and $T(+)$ for the onset and end of melting, respectively, and a value for the cooperative unit size. [20,38,41].

The temperature data are then used for the construction and the simulation of the phase diagrams. A four parameter model was used as described before, taking into account the asymmetry of the mixing behaviour. This yields two non-ideality parameters ρ_1 and ρ_2 for each phase [20].

4. Results

4.1. Pure components

The results for the thermodynamic data of the phospholipids are in agreement with previous data [42–45]. The results shown for measurements at extreme pH (DMPG/DPPG at pH 2 and DMPA/DPPA at pH 12) are from the first heating scan where no lipid degradation is detected (see Section 2).

4.2. Pseudobinary systems

In Figs. 1–5, DSC thermograms for the different pseudobinary systems are shown. The solid lines are the experimentally measured curves, the dotted lines are the simulated heat capacity curves cp^{sim} for the main transition. The measurements were performed in the temperature range of 8–85°C, but only the range in which a transition is observed is shown.

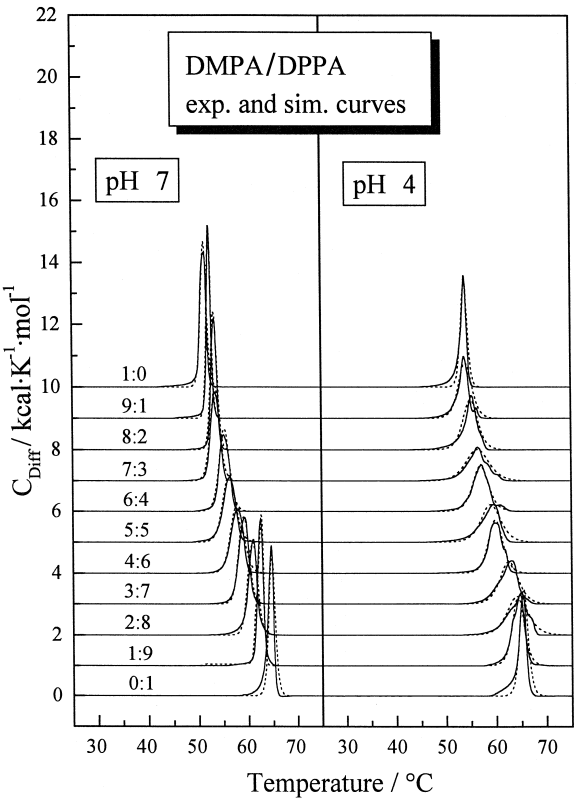

Fig. 1. DSC heating thermograms for DMPA/DPPA mixtures at various molar ratios at pH 7 and pH 4: Experimental cp-curves: solid line, simulated cp-curves: dotted line.

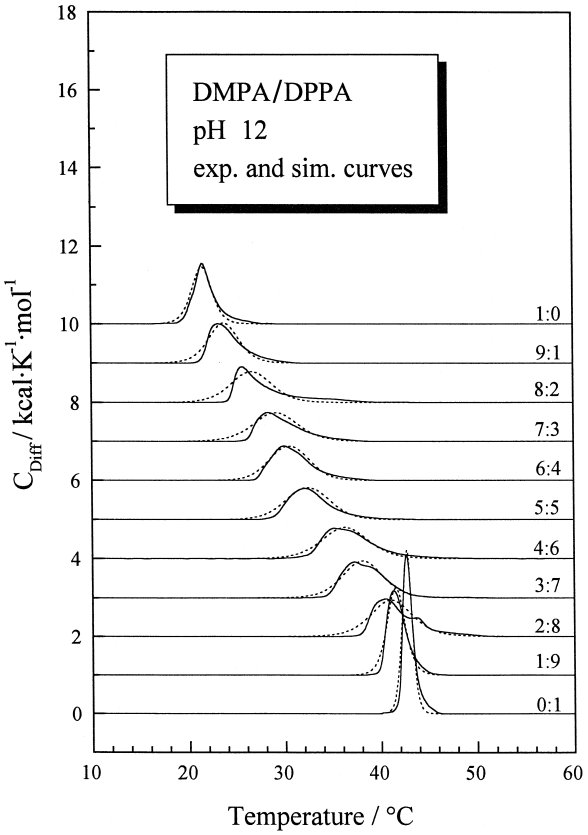

Fig. 2. DSC heating thermograms for DMPA/DPPA mixtures at various molar ratios at pH 12: Experimental cp-curves: solid line, simulated cp-curves: dotted line.

In all cases, the simulation of the DSC curves of the main phase transition of the DMPX/DPPX mixtures (X = different headgroup, X = A, C, E, G) gives satisfactory fits to the experimental curves.

The simulation of the DSC thermograms yields the temperatures which describe the beginning ($T(-)$) and end ($T(+)$) of melting of the bilayer system. These temperatures $T(-)$ and $T(+)$ are plotted in Figs. 6–10 (triangle up and down). Based on these temperature data, the phase diagrams were then recalculated and fitted by non-linear least square procedures using the four-parameter model described before [20,38]. The values obtained from the simulations are indicated in Figs. 6–10, including the differences in the non-ideality parameters between liquid-crystalline and gel phase $\Delta\rho_1 = \rho_{l1} - \rho_{g1}$ and $\Delta\rho_2 = \rho_{l2} - \rho_{g2}$, the latter value describing the difference in asymmetry between the liquid-crystalline and the gel phase. In Figs. 6–10, we have also added the temper-

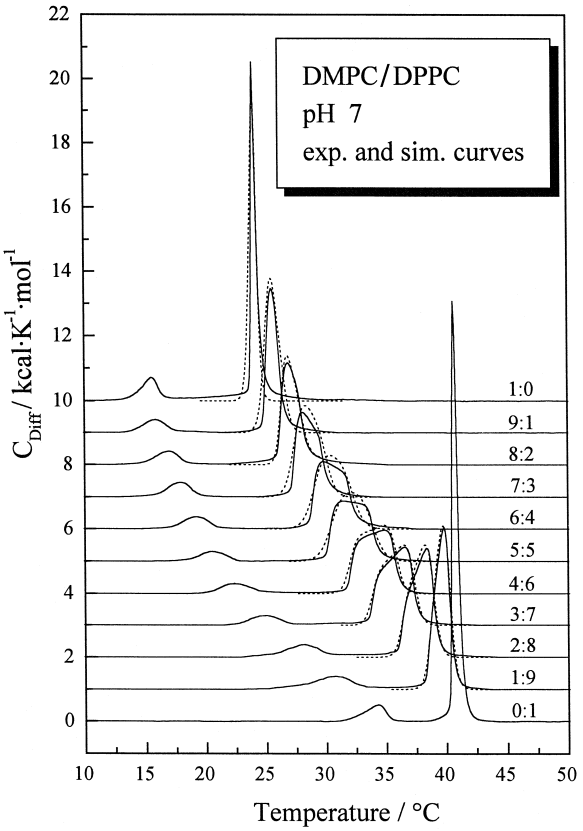

Fig. 3. DSC heating thermograms for DMPC/DPPC mixtures at various molar ratios at pH 7: Experimental cp-curves: solid line, simulated cp-curves: dotted line.

atures for onset and end of melting obtained by the usual empirical procedure (dots in the Figs. 6–10) [24,34,38,40]. These are clearly different in many cases.

The two non-ideality parameters for the gel phase (ρ_g) and for the liquid-crystalline phase (ρ_l) obtained from the simulation of the individual DSC peaks show a clear composition dependence. This is similar compared to the *x*-dependence obtained from the simulation of the total phase diagrams. The latter values are shown in Fig. 11 as a function of composition. The cooperative unit size c.u. is an additional parameter obtained from the simulations of the DSC peaks. The c.u. values are also composition dependent as shown in Fig. 12.

4.2.1. DMPA / DPPA

4.2.1.1. pH 7. The thermograms for DMPA/DPPA at neutral pH (Fig. 1, left panel) where PAs are singly charged [45], show one transition (L_β to L_α). The phase diagram of this system is represented in Fig. 6. The temperatures $T(-)$ and $T(+)$ obtained by the simulation of the heat capacity curves give a phase diagram with a narrower coexistence range compared to the temperature data obtained by the empirical method (this is usually the case) [38,40]. The $\Delta\rho$ values are negative and decrease with increasing amount of DPPA. The simulation of the phase diagram (Fig. 6) gives positive ρ_1 values with $\rho_{g1} = +426$ cal/mol and $\rho_{l1} = +263$ cal/mol, i.e., $\rho_g > \rho_l > 0$. DMPA/DPPA at pH 7 is the only system having a positive ρ_{l1} value, whereas all other systems at this pH have a negative (DMPE/DPPE) or vanishing non-ideality parameter ρ_{l1} (DMPC/DPPC and DMPG/DPPG). The asymmetry of mixing for this system is negligible (see Fig. 11).

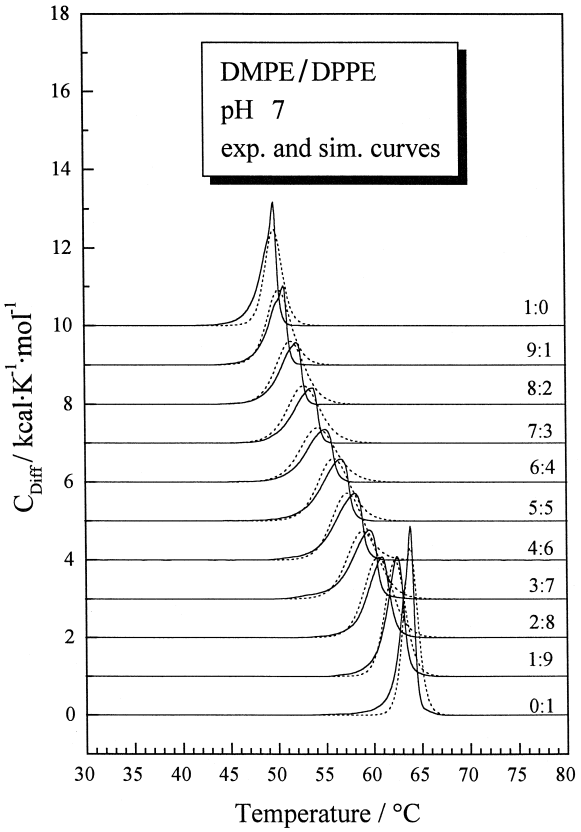

Fig. 4. DSC heating thermograms for DMPE/DPPE mixtures at various molar ratios at pH 7: Experimental cp-curves: solid line, simulated cp-curves: dotted line.

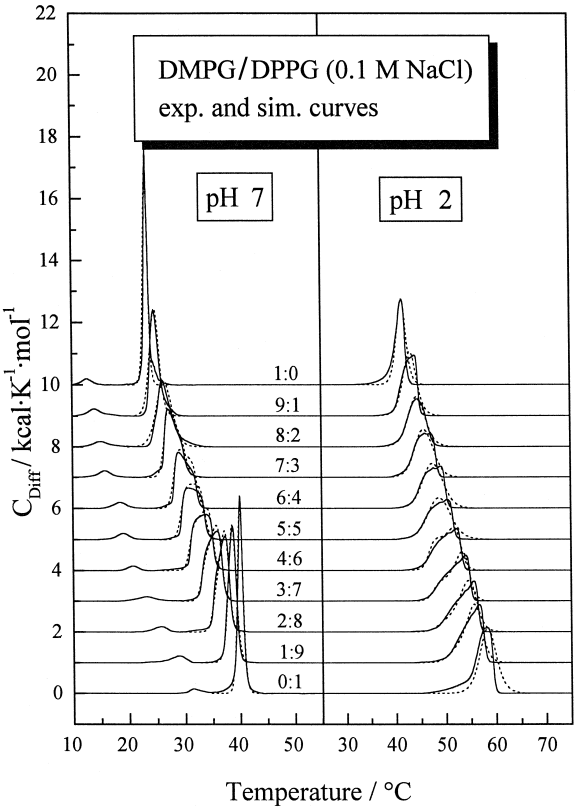

Fig. 5. DSC heating thermograms for DMPG/DPPG mixtures at various molar ratios at pH 7 and pH 2: Experimental cp-curves: solid line, simulated cp-curves: dotted line.

4.2.1.2. pH 4. At pH 4, PAs are partly protonated [43,45]. The thermograms are slightly broader and more structured (Fig. 1, right). The simulation of the phase diagrams gives negative non-ideality parameters with values of -500 to -600 for ρ_1 and strong negative asymmetry terms for both phases. Again, $\rho_{g1} > \rho_{l1}$, but the difference of both non-ideality parameters is smaller ($\Delta\rho_1 = -72$ cal/mol) compared to the same system at pH 7 ($\Delta\rho_1 = -163$ cal/mol) (see Fig. 11).

4.2.1.3. pH 12. At pH 12, PAs have a doubly negative charged headgroup [43,45]. The increased electrostatic repulsion and the impossibility for the formation of a hydrogen bonding network between the headgroups leads to strong reduction of the transition temperature. The thermograms at pH 12 are much broader compared to DSC curves at neutral pH. The curves show a relatively sharp increase of the heat capacity and the end of melting is characterised by a long and smooth decrease of cp (Fig. 2). At low amounts of DPPA $\Delta\rho$ is negative (~ -80 cal/mol) and increases to $+100$ cal/mol with increasing amount of DPPA. Again we have negative values for the non-ideality parameters with ρ_{g1} and $\rho_{l1} \sim -230$ cal/mol ($\Delta\rho_1 = +4$ cal/mol). The asymmetry term is more pronounced for the gel phase than for the liquid-crystalline phase with $\rho_{g2} = -265$ cal/mol and $\rho_{l2} = -146$ cal/mol which leads to $\Delta\rho_2 = +119$ cal/mol (see Fig. 11).

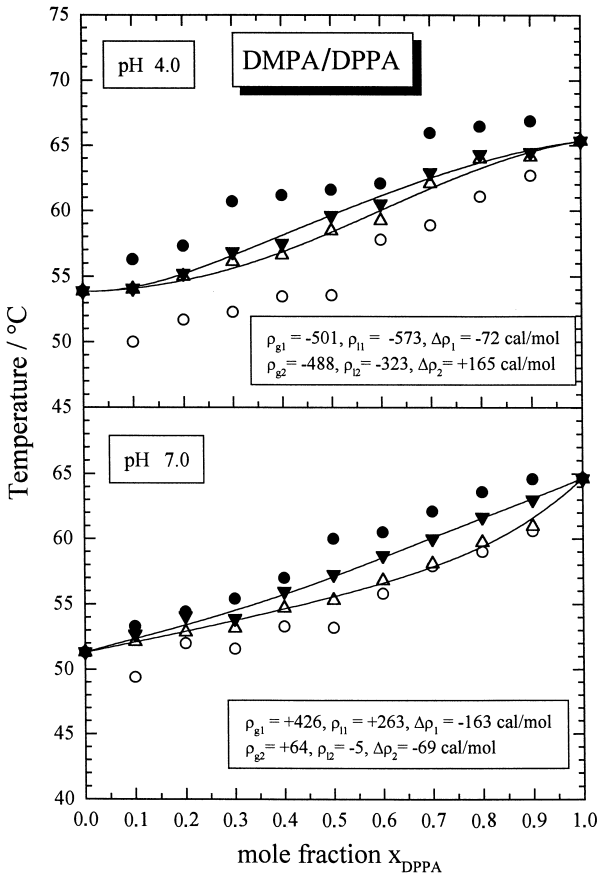

Fig. 6. Pseudobinary phase diagrams for DMPA/DPPA mixtures at pH 4 and pH 7. $T(-)$ and $T(+)$ were obtained from the simulation of the cp-curves (up and down triangles), the open and filled circles are $T(-)$ and $T(+)$ values obtained by the usual empirical procedures. The coexistence lines were calculated using the four parameter model for non-ideal, non-symmetric mixing as described in the text. The non-ideality parameters were obtained from a non-linear least square fit of the experimental data (up and down triangles).

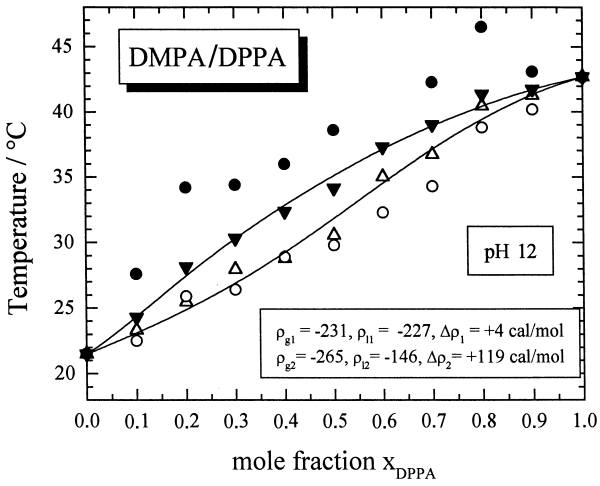

Fig. 7. Pseudobinary phase diagram for DMPA/DPPA mixtures at pH 12. $T(-)$ and $T(+)$ were obtained from the simulation of the cp-curves (up and down triangles), the open and filled circles are $T(-)$ and $T(+)$ values obtained by the usual empirical procedures. The coexistence lines were calculated using the four parameter model for non-ideal, non-symmetric mixing as described in the text. The non-ideality parameters were obtained from a non-linear least square fit of the experimental data (up and down triangles).

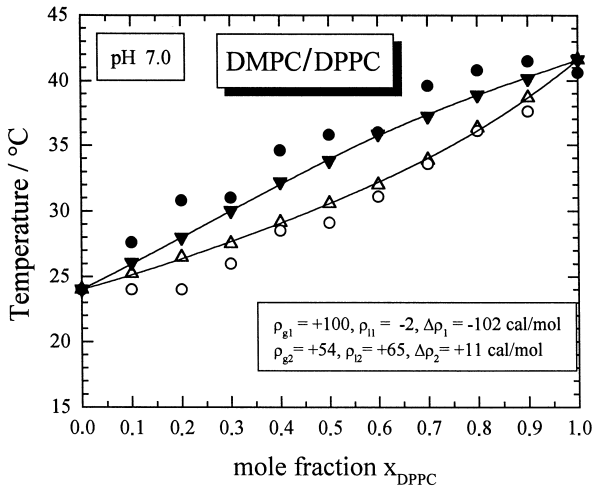

Fig. 8. Pseudobinary phase diagram for DMPC/DPPC mixtures at pH 7. $T(-)$ and $T(+)$ were obtained from the simulation of the cp-curves (up and down triangles), the open and filled circles are $T(-)$ and $T(+)$ values obtained by the usual empirical procedures. The coexistence lines were calculated using the four parameter model for non-ideal, non-symmetric mixing as described in the text. The non-ideality parameters were obtained from a non-linear least square fit of the experimental data (up and down triangles).

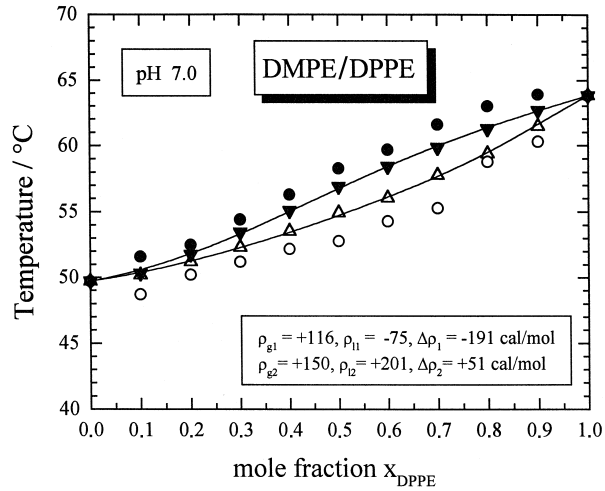

Fig. 9. Pseudobinary phase diagram for DMPE/DPPE mixtures at pH 7. $T(-)$ and $T(+)$ were obtained from the simulation of the cp curves (up and down triangles), the open and filled circles are $T(-)$ and $T(+)$ values obtained by the usual empirical procedures. The coexistence lines were calculated using the four parameter model for non-ideal, non-symmetric mixing as described in the text. The non-ideality parameters were obtained from a non-linear least square fit of the experimental data (up and down triangles).

4.2.2. DMPC / DPPC

4.2.2.1. pH 7. The DSC curves of the system DMPC/DPPC are plotted in Fig. 3. Two transitions are observed, namely a gel to gel transition ($L_{\beta'}$ to $P_{\beta'}$) and a gel to liquid-crystalline transition ($P_{\beta'}$ to L_{α}) [51]. Both phase transitions are well separated from each other, so that good simulations of the main transition are obtained (dotted curves in Fig. 3). As expected, the calculated non-ideality parameters are higher for the gel phase compared to the values for the fluid phase. The simulation of the phase diagram shows that mixing is almost ideal, ρ_{g1} is only slightly positive with +100 cal/mol, whereas for the fluid phase ρ_{l1} vanishes. The asymmetry terms are very small for both phases (see Fig. 11).

4.2.3. DMPE / DPPE

4.2.3.1. pH 7. The thermograms for the PEs (Fig. 4) are in general broader compared to those of PCs (Fig. 3). The non-ideality parameters obtained from the

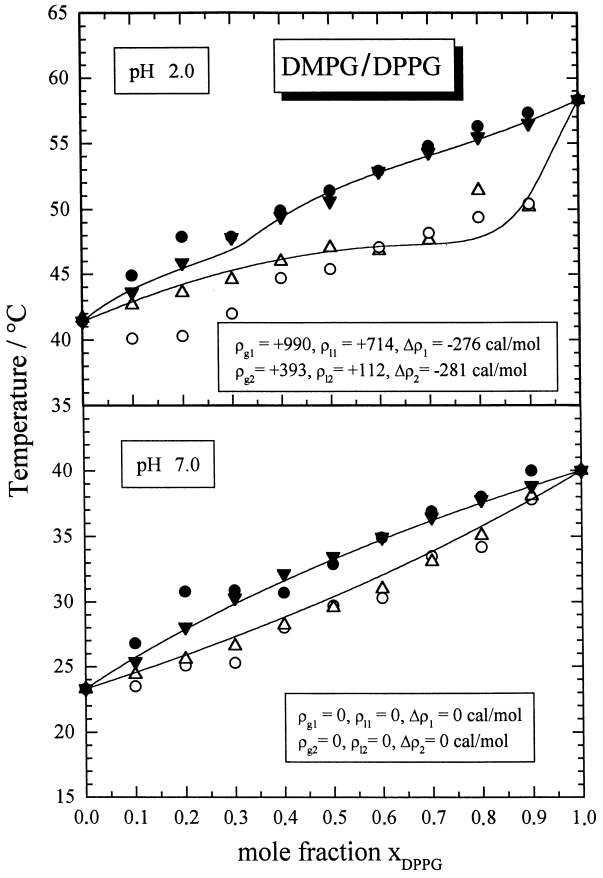

Fig. 10. Pseudobinary phase diagrams for DMPG/DPPG mixtures at pH 2 and pH 7. $T(-)$ and $T(+)$ were obtained from the simulation of the cp curves (up and down triangles), the open and filled circles are $T(-)$ and $T(+)$ values obtained by the usual empirical procedures. The coexistence lines were calculated using the four parameter model for non-ideal, non-symmetric mixing as described in the text. The non-ideality parameters were obtained from a non-linear least square fit of the experimental data (up and down triangles).

simulation of the cp-curves are all positive with $\rho_g > \rho_1$ which leads to a negative $\Delta\rho$ value. Increasing amount of DPPE increases $\Delta\rho$, but it still remains negative. The simulation of the phase diagram gives a positive value of $+116$ cal/mol for ρ_{g1} and a negative ρ_{l1} of -75 cal/mol which also leads to a negative $\Delta\rho_1$ of -191 cal/mol. Both asymmetry terms are positive (see Fig. 11).

4.2.4. DMPG / DPPG

4.2.4.1. pH 7. The thermograms for the system DMPG/DPPG are shown in Fig. 5 and are very similar to those of the analogous PC mixtures. Both systems have a pretransition and the shape of the main phase transition peaks shows the same tendency with increasing amount of the lower melting component. The simulated phase diagram has an ideal lens-like shape with all non-ideality parameters being zero.

4.2.4.2. pH 2. Protonation of the PGs increases the stability of the gel phase, the temperatures of the main transition are shifted to higher values, and the thermograms are slightly broader compared to those at pH 7. Particularly in the range of $x_{DPPG} = 0.4$ to 0.7 the coexistence range is relatively broad. The non-ideality parameters are now positive for both

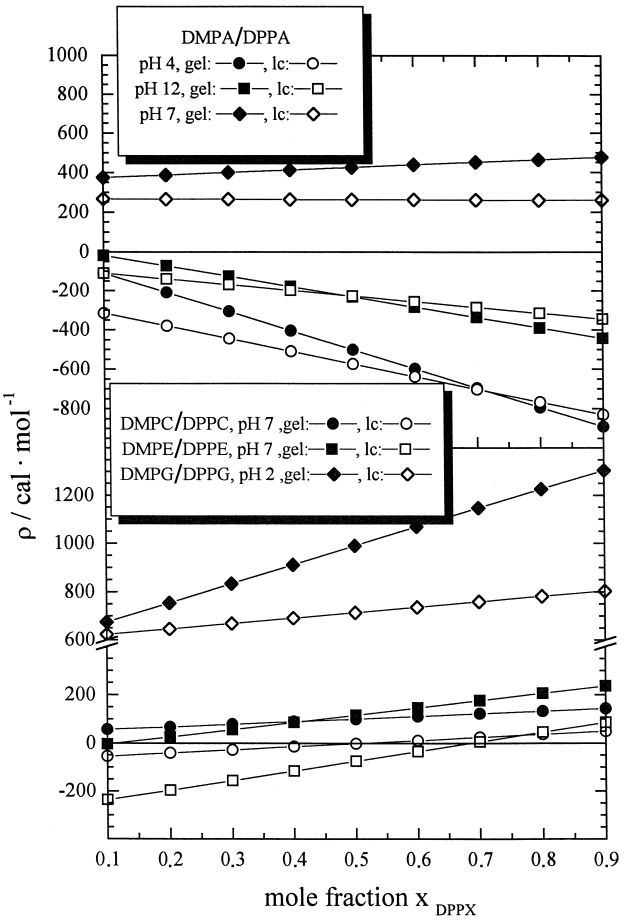

Fig. 11. Non-ideality parameter ρ as a function of composition, calculated from the values obtained by the simulations as shown in Figs. 6–10, i.e., $\rho = \rho_1 + \rho_2 \cdot (2x_{DPPX}\text{-}1)$. Open symbols: liquid-crystalline phase, filled symbols: gel phase.

phases and again $\rho_g > \rho_l$ leading to a negative $\Delta\rho$ with a considerable composition dependence. For low amounts of DPPG $\Delta\rho$ has a value of ~ -100 cal/mol which decreases to -600 cal/mol with increasing amount of DPPG. Particularly in the gel phase the tendency for demixing increases with high DPPG content (see Fig. 11).

5. Discussion

In order to clarify the details concerning the intermolecular interactions responsible for the mixing behaviour and to extract the factors governing the miscibility of different phospholipid species, it was desirable to investigate systematically selected combinations of two phospholipids such as those with same headgroup and different acyl chains and compare the results with those obtained for binary mixtures of lipids with different headgroups and also different chain lengths [20,34–38,40].

The DSC curves of the pseudobinary phospholipid mixtures were simulated with a thermodynamic model accounting for the non-ideal mixing in the gel as well as the liquid-crystalline phase as described before, where the broadening of the transition due to limited cooperativity was taken into account using a simple two state model with a cooperative unit size as adjustable parameter [20,38]. The simulated cp-curves are represented by dotted lines in the Figs. 1–5 and comparison with the experimental curves shows that the approach used gives relatively good results for these simple mixtures with low non-ideality. From the simulation of the heat capacity curves temperatures $T(-)$ and $T(+)$ for the beginning and end of the melting process of the transition were obtained (triangles up and down in the Figs. 6–10) and used for the simulation of the phase diagrams. Here, non-symmetric four parameter Bragg–Williams approximation was used. In almost all cases this approach leads to better fits than a symmetric mixing model [20]. The van't Hoff enthalpy obtained from the simulation of the cp-curves yields the cooperative unit size (c.u.) as a function of composition (Fig. 12). The c.u. reflects the number of molecules that change abruptly their physical state (gel to liquid-crystalline state). The analysis of Fig. 12 shows a general trend observed before for other mixtures, namely that the

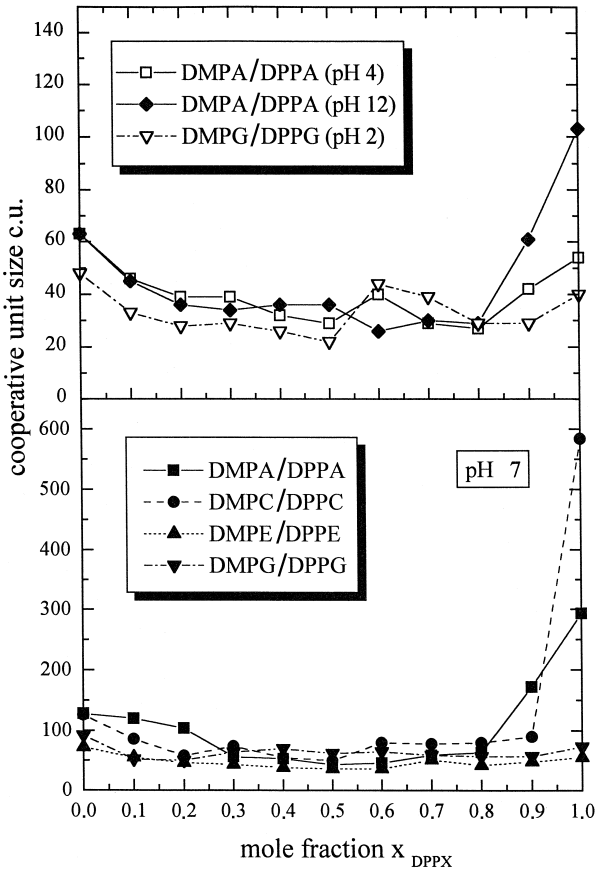

Fig. 12. Cooperative unit size (c.u.) for DMPX/DPPX mixtures as a function of composition at different pH-values.

cooperative unit size decreases in the mixtures compared to the pure compounds. This observation corresponds to suggestions based on model calculation of Sugár [41]. The 'U'-like shape of this curve has also been reported in our previous studies on phospholipid mixtures with different headgroups [20,38,40].

The non-ideality parameters derived from the simulations of the phase diagrams can be interpreted in terms of the difference in the pair-interaction energies between like pairs (A–A and B–B) and mixed-pairs (A–B) formed in the mixture. The non-ideality parameter ρ is defined as: $\rho = z \cdot [u_{AB} - 1/2 \cdot (u_{AA} + u_{BB})]$ where z is the first coordination number and u_{AA}, u_{BB} and u_{AB} the molar energies of A–A, B–B and A–B pair interactions [3,4,47]. For ideal mixing, the intermolecular interaction of A–A or B–B-pairs are equal to that of a mixed-pair A–B, the non-ideality parameters are consequently zero. The sign of ρ refers to different kinds of pair formations. A positive

ρ means that the mixed pair formation in the mixture is energetically less favourable than the like pair formation. A positive non-ideality parameter therefore reflects the tendency of clustering of like molecules whereas negative ρ values indicate mixed pair formation is more likely [38,40,52].

5.1. Pseudobinary systems at pH 7

In all cases where both lipids have identical headgroups we found that $\rho_{g1} \geq \rho_{l1}$. This means that the liquid-crystalline bilayer exhibits a higher miscibility than the gel phase bilayer regardless of the type of lipid headgroup (DMPG/DPPG shows ideal mixing). Furthermore, $\rho_{g1} > 0$ indicates clustering of like molecules with the following trend: $\rho_{g1}(\mathrm{PA}) > \rho_{g1}(\mathrm{PE}) > \rho_{g1}(\mathrm{PC}) > \rho_{g1}(\mathrm{PG})$. Similar results have been obtained by Nibu et al. [34] for a series of homologous lipids with different acyl chain lengths. However, their values for the non-ideality parameters are much larger due to the different method for determining the temperatures for onset and end of melting. They used the conventional method which leads to phase diagrams with a wider separation of the coexistence lines. This can be seen in Figs. 1–5, where we have included the temperature values obtained by the usual empirical procedure.

The non-ideality parameters for the liquid-crystalline phase are generally less positive so that the difference $\Delta\rho = \rho_l - \rho_g = \Delta\rho_1 + \Delta\rho_2 \cdot (2 \cdot x - 1)$ is negative over the whole mole fraction range with the exception of the PG mixture, which behaves ideally. In the case of DMPC/DPPC and DMPE/DPPE, the asymmetry terms ρ_2 are slightly positive for both phases, meaning that the mixtures become less ideal with increasing content of the longer chain compound.

In a first approximation, the observed non-ideality parameter can be separated into one contribution arising from non-ideal headgroup interactions (ρ_{hg}) and another, which arises from non-ideal mixing of the hydrocarbon chains (ρ_c). The mixtures studied here, however, are composed of two lipids with identical headgroups, so that the pair interaction energies arising from the headgroups are the same for like and unlike pairs and cancel in the calculation using the Bragg–Williams approximation, i.e., $\rho_{hg} = z \cdot [u_{ABhg} - 1/2 \cdot (u_{AAhg} + u_{BBhg})] = 0$. Therefore, all observed non-ideality effects should in this approximation arise from differences in interaction energies of the hydrocarbon chains. Because in all four systems the chain length differences are the same, one would expect similar or even identical non-ideality parameters for all four mixtures. This is evidently not the case.

The question is then, how to interpret these differences. The chemical structure and size of the headgroup determines the type of gel phase that is formed for a given chain length. PCs [46] and PGs form $P_{\beta'}$-phases below their main phase transition temperature, whereas PEs form an L_β-phase. PAs seem to adopt an ordered phase with a slight tilt angle of 5–10° [48]. Thus there are notable differences in structure for the phase existing just below the main phase transition for the different phospholipid classes. These are due to the differences in headgroup size, hydration, and intermolecular attractive headgroup interactions. For PEs and PAs it is well known that attractive hydrogen bonds can be formed between the headgroups. The attractive headgroup interactions between PEs and PAs are therefore much larger than between PC or PG headgroups, where theses H-bonds seem to be absent. These differences in headgroup interactions are retained in the L_α-phase, so that also for the fluid phase differences in packing density are observed, depending on headgroup type. PEs and PAs have more densely packed liquid-crystalline phases than PCs and PGs, as shown by ^{2}H NMR investigations [49–52]. The larger ρ values for PA and PE are therefore a consequence of stronger and not lower attractive headgroup interactions, as suggested by Nibu et al. [34].

In pure systems, the interaction energies between the hydrocarbon chains are therefore dependent on the type of headgroup and the type of gel phase formed below the main transition temperature. For $P_{\beta'}$-phases one can expect lower van der Waals interaction energies because the molecules are already in a slightly disordered state. For L_β-phases, the van der Waals interaction energies are expected to be larger because the all–trans hydrocarbon chains are in register parallel to each other at closer distance. For PEs and PAs one would therefore expect larger non-ideality parameters for the gel phase than for PCs and PGs. These expectations are corroborated by the experimental ρ_{g1} values for the gel phase found from

the simulations of the phase diagrams. These values are positive with the following order for the four mixtures: PAs > PEs > PCs > PGs.

For the liquid-crystalline phase, one would expect a similar order. This is only partly observed, for DMPE/DPPE a negative ρ_{l1} is found, which seems to indicate clustering of unlike molecules. This is not very likely, the negative value seems to be due to the fact that the coexistence curves are more sensitive to the difference in non-ideality parameters $\Delta\rho$ than to the absolute values [20]. The $\Delta\rho$ values should show the same trend as the absolute values of the non-ideality parameters. We indeed observe the following expected sequence for the absolute values of $\Delta\rho_1 = \rho_{l1} - \rho_{g1}$: PEs > PAs > PCs > PGs.

For all mixtures, except DMPG/DPPG, we find slightly asymmetric mixing behaviour. For gel phase mixtures the asymmetry parameters ρ_{g2} are positive, indicating that the mixture becomes less ideal with increasing mole fraction of the longer chain component. This means that short chain analogues introduced into a gel phase of the longer chain analogue have a larger tendency to cluster than when a longer chain lipid is incorporated into the gel phase of the shorter chain analogue. This effect seems also to be retained for the liquid-crystalline phases, but to a lesser extent.

5.2. The influence of headgroup charge

For the two binary mixtures DMPA/DPPA and DMPG/DPPG we also investigated the influence of a change in headgroup charge on the miscibility properties. Lowering the pH, leads in both cases to a partial protonation of the PA or PG headgroup, respectively. This reduces electrostatic repulsion, changes the hydration properties, and increases the possibility for an intermolecular hydrogen bonding network between the lipid headgroups. As a consequence, the properties of the lammellar phases are also changed. For PGs, the tilt angle is reduced upon protonation [53–55]. For PAs, similar effects can be expected. The packing density of the liquid-crystalline phase is probably also dependent on the degree of protonation [55]. In the case of PAs, changing the pH to 12 induces the dissociation of the second proton and the headgroups become doubly charged. The molecular packing in the gel phase bilayers changes, the tilt angle increases [48] and in the L_α-phase the molecules are less densely packed compared to the packing at pH 7 as determined by ^2H NMR-spectroscopy [51].

5.2.1. DMPA / DPPA

At pH 4, the headgroups carry -0.5 to -0.6 elementary charges [42,43,45]. The non-ideality parameters have large negative values and ρ_{g1} and ρ_{l1} differ only slightly. The asymmetry terms of the non-ideality parameters are also negative for both phases (see Fig. 11) and much larger than for the system at pH 7, resulting in a slightly S-shaped phase diagram (see Fig. 6). The negative sign of both ρ values indicates that the formation of mixed pairs is favoured.

Negative ρ values are also found for DMPA/DPPA at pH 12, but the values are smaller. The asymmetry term for the non-ideality parameters are again negative. At pH 12, PAs have a doubly negative charged headgroup. An intermolecular hydrogen bonding network cannot be formed and the electrostatic repulsion between the headgroups and their hydration are increased. Furthermore, the angle of tilt of the hydrocarbon chains of the PAs in the gel phase increases with headgroup charge reducing the van der Waals interactions between the chains [48].

The analysis of the phase diagrams at pH 4 and pH 12 leads to the conclusion that in both cases pair formation between unlike molecules is favourable and that with increasing DPPA content the mixtures become less ideal in the sense that pair formation between unlike molecules increases. At low DMPA content the mixtures behave almost ideally. This mixing behaviour is quite different from the one observed at pH 7 and again shows, that headgroup interactions are strongly influencing the mixing behaviour. Why pair formation of unlike molecules is favoured for partly protonated and for doubly charged PAs and not for singly charged PAs is unclear at present.

5.2.2. DMPG / DPPG

At pH 2, the PG headgroups are approximately 90% protonated under our experimental conditions.

The mixing properties change drastically compared to the mixtures at pH 7. The non-ideality parameters all become positive and also the asymmetry parameter are positive, indicating an increased demixing with increasing DPPG content. Considering the miscibility in the gel phase we have to take into account that protonation decreases the tilt angle from 30° relative to the bilayer normal in the charged state at pH 7 to less than 5° at pH 1–2 (data for DPPG at 20°C from [54]). This reduction in tilt angle increases the van der Waals interactions between the chains and leads to a better chain packing. This is probably the reason for the positive ρ values for the gel phase, i.e., the tendency for clustering of like molecules.

For liquid-crystalline bilayers, the fluidity was found to be greater for negatively charged PGs compared to the fluidity of protonated PGs [55]. Apparently, the more condensed liquid-crystalline state formed by protonated PG again increases the van der Waals interactions between the chains and favours clustering of lipids with identical chain lengths, the ρ values becoming much more positive than at pH 7.

6. Summary and conclusions

The effects of headgroup structure and charge on the miscibility of saturated phospholipids with identical headgroups but different acyl chain lengths were investigated by DSC. The pseudobinary phase diagrams were constructed and analysed using a new procedure described recently [20,38,40]. The temperature values $T(-)$ and $T(+)$ describing the onset and end of the phase transition obtained by our method lead to phase diagrams with narrower coexistence regions as those obtained by the usual empirical procedure and therefore to lower non-ideality parameters as reported before.

Furthermore, the non-ideality parameters obtained by the simulation of the heat capacity curves showed that these parameters generally depend on the mixing ratio. This means that non-symmetric mixing behaviour is the rule. The analysis of the phase diagrams using a four parameter model for non-symmetric mixing in both phases supported these findings. In almost all cases the non-ideality parameter ρ_g for the gel phase is more positive than the corresponding non-ideality parameter ρ_l for the liquid-crystalline phase. This is not surprising, because steric effects play the major role for gel phase miscibility. These effects are reduced for liquid-crystalline bilayers, so that the miscibility becomes more ideal.

The systems analysed all have the same headgroup, only the chain length differs by two methylene units. One would assume that the mixing behaviour is solely determined by the difference in hydrocarbon chain length, so that all mixtures should behave similarly. This is not observed. For gel phase bilayers, the tendency $\rho_g(PA) > \rho_g(PE) > \rho_g(PC) > \rho_g(PG)$ was found indicating that the structure of the gel phase below the main phase transition temperature T_m has an influence on the mixing properties, i.e., lipids with strong intermolecular attractive headgroup interactions via hydrogen bonds, which form untilted L_{β}-gel phases (PE, PA) show larger deviations from ideal mixing than those forming $P_{\beta'}$-phase below T_m, such as PC and PG. Interestingly, changes in headgroup charge can lead to large changes in mixing behaviour, which cannot be explained satisfactorily on the basis of changes in gel phase structure, i.e., change in chain tilt, at the present time. Particularly the negative non-ideality parameters found for mixtures of partly protonated and for doubly negative charged PAs, indicating preferential mixed pair formation, are puzzling and need to be further investigated by other independent experiments.

Acknowledgements

We thank L. Mennicke for supplying us with the simulation programs for the cp curves and C. Johann for the intense and helpful discussions. This work was supported by the Deutsche Forschungsgemeinschaft (Bl 182/7-3) and the Fonds der Chemischen Industrie.

References

[1] S.J. Singer, G.L. Nicolson, Science 175 (1972) 720–731.
[2] M. Bloom, E. Evans, O.G. Mouritsen, Q. Rev. Biophys. 24 (1991) 293–313.
[3] A.G. Lee, Prog. Biophys. Molec. Biol. 29 (1975) 3–56.
[4] A.G. Lee, Biochim. Biophys. Acta 413 (1975) 11–23.
[5] A.G. Lee, Biochim. Biophys. Acta 472 (1977) 237–281.
[6] A.G. Lee, Biochim. Biophys. Acta 472 (1977) 285–344.
[7] A.G. Lee, Biochim. Biophys. Acta 507 (1978) 433–444.

[8] A.G. Lee, N.J.M. Birdsall, J.C. Metcalfe, P.A. Toon, G.B. Warren, Biochemistry 13 (1974) 3699–3705.
[9] J.E. Cronan, E.P. Gelman, Bact. Rev. 39 (1975) 232–256.
[10] T. Berclaz, M. Geoffroy, Biochemistry 23 (1984) 4033–4037.
[11] T. Berclaz, H. McConnell, Biochemistry 23 (1981) 635–6640.
[12] G. Benga, R.P. Holmes, Prog. Biophys. Molec. Biol. 43 (1984) 195–257.
[13] M. Glaser, Curr. Opin. Struct. Biol. 3 (1993) 475–481.
[14] W.L.C. Vaz, Biophys. Chem. 50 (1994) 139–145.
[15] W.L.C. Vaz, Mol. Membrane Biol. 12 (1995) 39–43.
[16] T.N. Metcalf, J.L. Wang, M. Schindler, Proc. Natl. Acad. Sci. U.S.A. 83 (1986) 95–99.
[17] P.F.F. Almeida, W.L.C. Vaz, T.E. Thompson, Biophys. J. 64 (1993) 399–412.
[18] A. Carruthers, D.L. Melchior, Biochemistry 22 (1983) 5797–5807.
[19] P.P.F. Almeida, W.L.C. Vaz, in: R. Lipowsky, E. Sackmann (Eds.), Structure and Dynamics of Membranes, Elsevier, Amsterdam, 1995, pp. 305–357.
[20] C. Johann, P. Garidel, L. Mennicke, A. Blume, Biophys. J. 71 (1996) 3215–3228.
[21] E.J. Shimshick, H.M. McConnell, Biochemistry 12 (1973) 2351–2360.
[22] A. Blume, Th. Ackermann, FEBS Lett. 43 (1974) 71–75.
[23] S.H. Wu, H.M. McConnell, Biochemistry 14 (1975) 847–854.
[24] S. Mabrey, J.M. Sturtevant, Proc. Natl. Acad. Sci. U.S.A. 73 (1976) 3862–3866.
[25] E.J. Luna, H.M. McConnell, Biochim. Biophys. Acta 470 (1977) 303–316.
[26] R. Mendelsohn, C.C. Koch, Biochim. Biophys. Acta 598 (1980) 260–271.
[27] K. Arnold, A. Lösche, K. Gawrisch, Biochim. Biophys. Acta 645 (1981) 143–148.
[28] J.W. Brauner, R. Mendelsohn, Biochim. Biophys. Acta 861 (1986) 16–24.
[29] A. Blume, Physical properties of biological membranes and their functional implications, in: C. Hidalgo, (Ed.), Plenum, New York, 1988.
[30] S. Ali, H.-N. Lin, R. Bitman, C.-H. Huang, Biochemistry 28 (1989) 522–528.
[31] H.D. Dörfler, G. Brezesinski, P. Miethe, Chem. Phys. Lipids 48 (1988) 245–254.
[32] A. Blume, Thermochim. Acta 193 (1991) 299–347.
[33] I.V. Polozov, J.G. Molotkovsky, L.D. Bergelson, Chem. Phys. Lipids 69 (1994) 209–218.
[34] Y. Nibu, T. Inoue, I. Motoda, Biophys. Chem. 56 (1995) 273–280.
[35] Y. Nibu, T. Inoue, Chem. Phys. Lipids 76 (1995) 159–169.
[36] T. Inoue, T. Tasaka, R. Shimotowa, Chem. Phys. Lipids 63 (1992) 203–212.
[37] T. Inoue, Y. Nibu, Chem. Phys. Lipids 76 (1995) 171–179.
[38] P. Garidel, C. Johann, A. Blume, Biophys. J. 72 (1997) 2196–2210.
[39] T. Inoue, Y. Nibu, Chem. Phys. Lipids 76 (1995) 181–191.
[40] P. Garidel, C. Johann, L. Mennicke, A. Blume, Eur. Biophys. J. 26 (1997) 447–459.
[41] I.P. Sugár, J. Phys. Chem. 91 (1987) 95–101.
[42] H. Träuble, H.J. Eibl, Proc. Natl. Acad. Sci. U.S.A. 71 (1974) 214–219.
[43] A. Blume, H.J. Eibl, Biochim. Biophys. Acta 558 (1979) 13–21.
[44] A.J. Verkleij, Biochim. Biophys. Acta 779 (1984) 43–63.
[45] A. Blume, J. Tuchtenhagen, Biochemistry 31 (1992) 4636–4642.
[46] M.J. Janiak, D.M. Small, G.G. Shipley, Biochemistry 15 (1976) 4575–4580.
[47] B. Tenchov, Prog. Surf. Sci. 20 (1985) 273–340.
[48] F. Jähnig, K. Harlos, H. Vogel, H. Eibl, Biochemistry 18 (1979) 1459–1468.
[49] P. Garidel, Diploma thesis, University of Kaiserslautern, Germany, 1993.
[50] W. Ziegler, A. Blume, Spectrochim. Acta Part A 51 (1995) 1763–1778.
[51] J. Tuchtenhagen, W. Ziegler, A. Blume, Eur. Biophys. J. 23 (1994) 323–335.
[52] W. Hübner, A. Blume, Ber. Bunsenges. Phys. Chem. 91 (1987) 1127–1132.
[53] A. Watts, K. Harlos, W. Maschke, D. Marsh, Biochim. Biophys. Acta 510 (1978) 63–74.
[54] A. Watts, K. Harlos, D. Marsh, Biochim. Biophys. Acta 645 (1981) 91–96.
[55] A. Watts, D. Marsh, Biochim. Biophys. Acta 642 (1981) 231–241.